

The influence of convection on the homogeneity of laser-applied coatings

H. J. HEGGE, J. TH. M. DE HOSSON

Department of Applied Physics, Materials Science Centre, University of Groningen, Nijenborgh 18, 9747 AG Groningen, The Netherlands

During laser alloying, a melt pool is created at the passage of a laser beam in which mixing occurs by convection because of surface tension gradients. This mixing process in the melt bath is reported here in different alloying elements on aluminium (manganese, nickel, cobalt) and steel (nickel) substrates and a homogeneous distribution did not appear to be evident. It is concluded that density differences, interface tensions and diffusion are the main factors affecting the mixing process.

1. Introduction

Nowadays surface alloying techniques are attracting more interest for practical applications. A promising process is laser surface alloying. A laser is scanned across a surface covered with powder. During passage a melt pool is created in which the surface layer is mixed with the substrate surface to obtain an improved microstructure at the surface. An important aspect is the homogeneity of the layer determining the reliability of the coating, especially if the coating is intended to be used in wear or corrosion-resistant applications.

Usually it is assumed that there exists perfect mixing in the melt pool [1]. In this work aspects of mixing are investigated and related to the convective flow in the melt pool. Because of the variation of the surface energy with temperature, a surface tension driven flow is created in the pool [2-4]. This flow takes up alloying elements or (ceramic) particles which are mixed with the molten material of the laser bath by diffusion and by centrifugal forces [5]. If there is insufficient time for these processes, a layered structure remains after resolidification.

A detailed study is made of manganese, nickel and cobalt on aluminium and nickel powder on iron. Powders and substrates are chosen because of their different melting points and densities.

2. Experimental procedure

The substrate material was ground and ultrasonically cleaned. Powder material of different compositions was deposited on it by making a suspension of the powder in methanol, submersing the sample in this suspension and evaporating the methanol. The coating material/substrate systems are listed in Table I.

The samples were scanned by the beam of a 1.5 kW CW-CO₂ laser (Spectra Physics 820) under an argon atmosphere. The laser passes were well separated to inhibit influences of adjacent laser scans. The Gaussian beam was deflected by a molybdenum mir-

ror and focused by a ZnSe lens with a focus distance of 127 mm. The focus point lay 5 mm above the surface. At the surface the power of the beam was 1300 W. The scanning velocities were between 1 and 25 cm sec⁻¹.

After the laser treatment, cross-sections were made of the different passes and were analysed by light microscopy, transmission electron microscopy (TEM) and scanning electron microscopy (SEM). Energy dispersive spectrometry (EDS) was also performed on the cross-sections to obtain information of the distribution of the different elements in the melt pool.

3. Theoretical model

Many studies have been devoted to the investigation of the convective flow in electric arc or laser weld pools [2-9]. It is generally accepted that the main reason for this flow is the gradient in the surface energy between the centre of the melt pool and the edges. The surface energy increases with decreasing temperature in pure liquid metals, which gives an outward directed flow at the surface [10]. The flow descends at the edges of the melt pool to the bottom whereas it rises again in the middle of the beam (see Fig. 1). The velocities at the surface are much higher than in lower parts of the pool. Sometimes a secondary convection cell was found in the lower parts of the melt pool especially at lower velocities [6]. If there are surface active elements such as oxygen and sulphur present, the surface energy gradient can be diminished or changed in sign. In the last case the surface flow is also reversed [5].

TABLE I Coating material/substrate systems used

	Substrate					
	Al	Al	Al	Al	Fe	Fe/0.2% C
Surface material	TiC	Mn	Co	Ni	Ni	TiC
Layer thickness (µm)	33	13	9	15	8	20.7

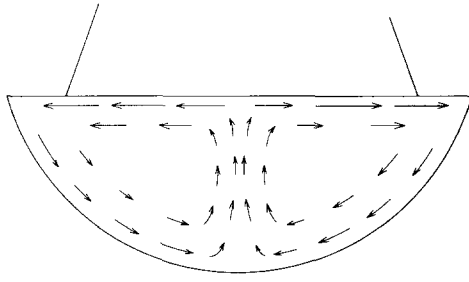


Figure 1 Convective flow in a cross-section of the melt pool. The velocity is indicated by the vectors.

Because heat flow is faster than the penetration of a velocity field in a fluid (thermal diffusion distance larger than flow diffusion distance), at the melt front the fluid velocity is very low, especially in the lower parts of this region [8]. At places with low thermal gradients, low fluid velocities are also found, e.g. at the edges and in the centre of the pool further away from the beam [11]. Because the convective velocity is determined by the temperature field it is not linearly dependent on the scan velocity [12].

Debate exists in the literature concerning the magnitude of the velocity in the melt. Numerical calculations give velocities, v , of the order of 0.1 to 10 m sec⁻¹ for aluminium [2, 5, 6, 12]. Analytical approximations using Anthony and Cline's model reveal velocities of 10 to 100 m sec⁻¹ for aluminium [4, 13].

In the former case, the Reynolds number is below 2000 if one uses the dimensions of the area of the pool where the highest velocities are found. In the latter, the melt pool would be very turbulent.

Let us consider a two-dimensional case: a cross-section of the laser pass. In the time w/v_c a volume of fluid flows across the surface, a layer of volume, V , melts

$$V = \left(\frac{w}{v_c}\right) v w d \quad (1)$$

where w represents the width of the melt bath and d is the depth. This volume replaces the fluid at the surface having a thickness, d_m ,

$$d_m = \frac{vd}{v_c} \quad (2)$$

In the case when the coating material has already melted and the interfacial energy is low or negative, the surface material behaves almost as part of the melt pool and the thickness, d_g , of a layer of this material will be at the end of the melt pool before it sinks

$$d_g = \frac{vd_1}{v_c} \quad (3)$$

where d_1 is the layer thickness.

If the surface material is heavier than the substrate material, due to gravity it will descend into the melt, provided it is not prohibited by interfacial tension, which means that the contact angle must be smaller than 90°. The depth, d'_g , to which material descends during passage is limited. The maximum distance a particle falls with a certain velocity is found by equating gravity and the friction forces in equilibrium in

the melt pool.

$$s = \frac{a\Delta\rho r^2 g}{18\eta} \Delta t \quad (4)$$

where $\Delta\rho$ is the difference in density, r the size of the descending volume, a a geometrical constant and Δt the time interval. If there is only diffusion in the surface layer, the distance travelled by coating elements in the melt will be

$$d_D = \left(\frac{Dw}{v_c}\right)^{1/2} \quad (5)$$

where D is the diffusion coefficient, and d_D the diffusion distance.

Because the convective velocity is many times higher than the laser scan velocity, a fluid element circulates many times in the melt pool before solidification and a periodic structure emerges with a period δ

$$\delta = d_m + d_g \quad (6)$$

After surface material has been taken up by the flow, the fluid will be homogenized by diffusion. The relaxation time, τ , for such a process is [14]

$$\tau = \frac{(\delta)^2}{\pi^2 D} \quad (7)$$

To obtain homogeneity by diffusion only, τ should be smaller than $1/v$, i.e. the average residence time a volume is in the melt bath.

If the density of the particles or droplets is equal to the density of the melted fluid only, the surface energy term determines if the powder is taken up in the stream. After pick up it will follow the streamlines.

Particles with different density will be displaced relative to the streamlines. However, if one calculates the maximum travel distance using the steady velocity found by equating the centrifugal forces with the friction forces, only small ($\ll 1 \mu\text{m}$) distances are found, which is in contrast to electron-beam melt pools [15].

Usually particles are entrapped at solidification, except at low velocities of the order of 10 to 100 $\mu\text{m sec}^{-1}$, when they can be pushed forward. Because the solidification velocity is larger than these values, only entrapment is expected [16, 17].

4. Results

Nickel, manganese and cobalt powders on aluminium and electro-deposition of nickel on iron were carried out. The samples were scanned by the laser at velocities between 1 and 25 cm sec⁻¹.

Three different types of distribution were found in the investigated systems:

- (i) completely dissolved material;
- (ii) "onion scale" type layers of alternating surface and substrate material (Fig. 2);
- (iii) irregularly formed areas of the surface material surrounded by substrate material.

The manganese on aluminium system did not show a completely homogeneous distribution. Manganese- and aluminium-rich layers are formed in an "onion

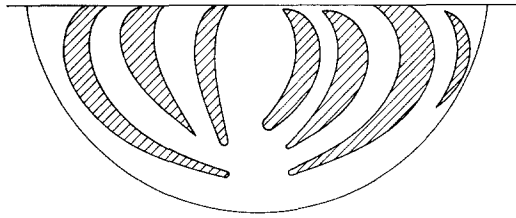


Figure 2 Schematic representation of a cross-section after a laser treatment without complete mixing. Areas with high concentrations of surface material are shaded.

scale” manner around the centre of the melt pool (Fig. 3).

Only at scan velocities of 1 cm sec^{-1} was an almost homogeneous melt pool formed. At higher velocities the number of scales decreased somewhat and the distinction between manganese-rich and aluminium-rich areas became clearer. After a subsequent laser pass at the same place, the mixing became better but at least three passes were necessary for the mixing to become homogeneous. After the second pass, distinct “onion scales” could no longer be detected but irregular manganese-rich areas were found (Fig. 4). The microstructure in the resolidified area was cellular/dendritic (cell size 1 to $10 \mu\text{m}$). Eutectic or featureless areas sometimes existed in the inhomogeneous laser passes, depending on the concentration.

The nickel and cobalt on aluminium both showed an almost homogeneous distribution after laser treatment at low velocities. Large onion-scale shaped Ni/Co rich areas were formed divided by small Ni/Co poor areas. At higher velocities, only small Ni/Co rich



Figure 4 Manganese on aluminium; cross-section after two laser passes at the same place. Scanning velocity 1 cm sec^{-1} .



Figure 3 Manganese on aluminium; “onion scale” type layers. Scanning velocity 10 cm sec^{-1} .

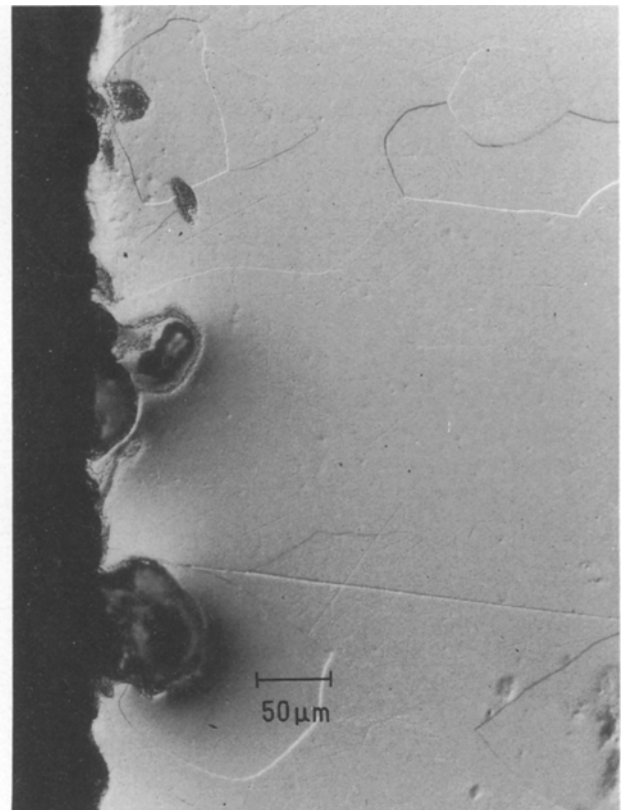


Figure 5 Cobalt on aluminium; some cobalt-rich areas were found in the upper parts of the laser-molten and resolidified area. Scanning velocity 40 cm sec^{-1} .

TABLE II Layer thicknesses and diffusion times compared with residence time, t_r , for manganese, nickel and cobalt on aluminium and nickel on iron. Experimental error in the measured quantities 30%, $w = 700 \mu\text{m}$, $D = 2 \times 10^{-9} \text{m}^2 \text{sec}^{-1}$

System	v (cm sec^{-1})	Depth (μm)	d_m (μm)	d_1 (μm)	d_g (μm)	d'_g (nm)	d_D (μm)	τ (ms)	t_r (m sec)
Mn/Al	1	300	3	10	0.1	10	1	0.5	70
	10	150	15	10	1	10	1	11.0	7
	20	150	30	10	2	10	1	51	3.5
Ni/Al	2.5	160	4	15	0.4	13	1	1	28
	10	110	11	15	1.5	13	1	8	7
Co/Al	1	150	1.5	9	0.1	13	1	0.1	70
	10	150	15	9	1.5	13	1	14	7
Ni/Fe	1.6	160	2.6	6	0.1	0.3	1	0.4	70

areas were formed, mostly at the surface. The concentration of Ni/Co in the enriched areas increased by tenths of a per cent with increasing scan velocity.

Laser melting of the nickel layer on iron produced a homogeneous microstructure: the fluctuations of the concentration were smaller than the accuracy of EDS measurements. At the edges of the laser passes, over a short distance (10 μm), in the cross-sections, a nickel layer was found at the bottom of the melted and resolidified area.

5. Discussion and conclusions

The experimental results can be explained by the model described. Table II shows the residence time compared with the necessary diffusion times. A convective velocity of 1m sec^{-1} was used and a diffusion coefficient of $2 \times 10^{-9} \text{m}^2 \text{sec}^{-1}$. From the upper limit for sinking of the coating material, it can be seen that this effect can be neglected.

Because liquid metals mix well, their interfacial energies are low and melted coating and substrate material will act as one liquid. At low velocities convection in the melt pool is large enough to create a homogeneous distribution of elements, especially in the system of nickel on iron. At higher velocities in the nickel on aluminium and the cobalt on aluminium system the available time is insufficient to homogenize the melt by dissolution and diffusion. For velocities of 20cm sec^{-1} and higher, the temperature in the melt pool was probably too low for nickel or cobalt to attain a sufficiently low viscosity. A simulation with pure aluminium revealed, as a comparison, that only a quarter of the surface had a temperature higher than 1800 K. This effect becomes more distinct if one considers the case of manganese on aluminium. Manganese has a lower melting point than nickel or cobalt. No large conglomerates of surface material were observed. Although there is insufficient time for dissolution, especially at higher velocities, the manganese is already distributed as onion scales throughout the pool. It is not a solidification effect, because in that case one would expect that after the second pass, a similar distribution, although fainter, would be found.

Thus the following conclusions are drawn.

1. Although usually a homogeneous distribution of surface material and substrate material is found during a laser treatment, inhomogeneities occur, which can be explained by a convective mixing model.

2. In this study (nickel, cobalt and manganese on aluminium, and nickel on iron) it was found that for

metals on a metallic substrate the take-up of the surface material presented no difficulties.

3. Mixing is mainly achieved by distribution of the material in the convective flow and by diffusion during laser treatment.

4. The larger the melting temperature between substrate and surface material, the worse the homogenization will be.

Acknowledgements

This work is part of the research programme of the Foundation for Fundamental Research on Matter (FOM-Utrecht), Foundation for Technical Sciences (STW-Utrecht) and has been made possible by financial support from the Netherlands Organization for Research (NWO-The Hague).

References

1. C. W. DRAPES and C. A. EWING, *J. Mater. Sci.* **19** (1984) 3815.
2. S. KOU and Y. H. WANG, *Met. Trans.* **17A** (1986) 2265.
3. J. A. SEKHAR, S. KOU and R. MEHRABIAN, *ibid.* **14A** (1983) 1169.
4. T. R. ANTHONY and H. E. CLINE, *J. Appl. Phys.* **48** (1977) 3888.
5. R. E. SUNDELL, H. D. SOLOMON and S. M. CORREA, in Proceedings of the Conference on Advances in Welding Science and Technology, Gatlinburg, Tennessee, USA, 18 to 22 May 1986 (ASM International) pp. 53-7.
6. S. KOU, D. K. SUN and Y. P. LE, *Met. Trans.* **14A** (1983) 643.
7. P. G. KLEMENS, *J. Appl. Phys.* **47** (1976) 2165.
8. H. E. CLINE, in Proceedings of the Conference on Lasers in Metallurgy, Chicago, Illinois, USA, 1981, 110th AIME meeting, edited by K. Mukherjee and J. Mazumder (Metallurgical Society, AIME, 1981) pp. 105-14.
9. T. R. ANTHONY and H. E. CLINE, *J. Appl. Phys.* **48** (1977) 3888.
10. B. C. ALLEN, in "Liquid Metals" edited by S. Z. Beer (Marcel Dekker, New York, 1972) pp. 161-204.
11. K. E. EASTERLING, *Mater. Sci. Engng* **65** (1984) 191.
12. C. CHAN, J. MAZUMDER and M. M. CHEN, *Met. Trans.* **15A** (1984) 2175.
13. P. A. MOLIAN, *Scripta Metall.* **16** (1982) 65.
14. D. A. PORTER and K. E. EASTERLING, "Phase Transformations in Metals and Alloys" (Van Nostrand Reinhold, Wokingham, 1981) p. 254.
15. T. TAUQIR, P. R. STRUTT and P. G. KLEMENS, *Mater. Sci. Engng.* **94** (1987) 251.
16. D. M. STEFANESCU, B. K. DHINDAW, S. A. KACAR and A. MOITRA, *Met. Trans.* **19A** (1988) 2847.
17. D. R. UHLMANN, B. CHALMERS and K. A. JACKSON, *J. Appl. Phys.* **35** (1964) 2986.

Received 17 November
and accepted 1 December 1989